

The Transport Properties of CO₂ and CH₄ for Chemically Modified Polysulfones

HYUN-JOON KIM,¹ SUK-IN HONG²

¹ Division of Advanced Industrial Engineering, Kyonggi University, San94-6, Yui-dong, Paldal-ku, Suwon, Kyonggi-do 442-760, Korea

² Department of Chemical Engineering, Korea University, 1,5-ka, Anam-dong, Sungbuk-ku, Seoul 136-701, Korea

Received 26 April 1999; accepted 5 August 1999

ABSTRACT: The sorption and transport properties of pure CO₂ and CH₄ for a series of polysulfones were measured. The effects of molecular structure of polysulfones on transport properties were studied using chemically modified polysulfones, including TMSPSF (bisphenol-A trimethylsilylated polysulfone), BPSF (bromobisphenol-A polysulfone), and BTMSPSF (bromobisphenol-A trimethylsilylated polysulfone). The effects of operating pressure on the sorption and permeation properties of polysulfones were examined. The permeation properties for a mixture of CO₂ and CH₄ were also measured and these results were compared with those obtained from the experiments of pure gases. The sorbed concentrations and permeability coefficients are well fitted to a conventional dual-mode model. The permeability coefficients of each gas of a binary mixture are lower than those of pure gases, which shows the competition effect between each component. The permeability coefficients of polysulfones rank in the following order, TMSPSF > BTMSPSF > bisphenol-A polysulfone (PSF) > BPSF. The effect of the substituents on chain packing was related to the gas-permeation properties. Fractional free volume (FFV) calculations and X-ray diffraction were used to judge chain packing. In comparison with PSF, the higher values of permeability coefficients for TMSPSF and BTMSPSF are due to higher FFV and *d* spacing. The lower permeability coefficients for BPSF is attributed to the strong induced dipole interchain interaction. Addition of bromo substituents to TMSPSF is also found to decrease the permeability coefficients for BTMSPSF, suggesting that the potential increase in FFV due to packing-disrupting bulky trimethylsilyl groups is overridden by the increase in cohesive energy density. © 2000 John Wiley & Sons, Inc. *J Appl Polym Sci* 76: 391–400, 2000

Key words: polysulfone; trimethylsilyl group; polar substituent; sorption; permeability

INTRODUCTION

Membrane-based gas-separation technology has emerged as an important alternative technology to cryogenic distillation or pressure swing adsorp-

tion. Commercial gas-separation membrane processes mainly utilize polymers due to processability. New polymeric materials with higher permeability and selectivity are required to advance membrane technology in the commercial areas. It is generally known that polymeric membrane which has high gas permeability exhibits low selectivity and vice versa.^{1,2} Careful molecular design of polymer structure can lead to materials that can run counter to a certain extent to this

Correspondence to: S.-I. Hong (sihong@kucncz.leorea.ac.krkr).

Journal of Applied Polymer Science, Vol. 76, 391–400 (2000)
© 2000 John Wiley & Sons, Inc.

trade-off relationship. Recent studies have focused on systematically varying polymer structure to increase permeability and selectivity and especially made attempts to introduce bulky and rigid substituents onto polymer.^{3–7} Structural changes that inhibit chain packing can increase permeability and those that reduce chain mobility can lead to higher selectivity.^{8,9}

Recently, some polymer materials containing silicon on the polymer branches such as poly(trimethylsilylmethyl methacrylate), poly(vinyl trimethylsilane), and poly(trimethylsilyl propyne) are well recognized as promising membrane materials.^{10,11} These materials have exceptionally high permeabilities, but the disadvantage of these polymers is their low selectivities. Our previous study also described that trimethylsilylated polysulfone had higher permeability than polysulfone, but showed lower selectivity.¹²

Muruganandam et al. reported that chloro and bromo substitutions onto polycarbonate increased gas selectivities.¹³ By considering this fact, this present work involves the synthesis of bromobisphenol-A trimethylsilylated polysulfone (BTMSPSF), in which phenyl rings of bisphenol and sulfone units in polysulfone are substituted with bromine and trimethylsilyl groups, respectively.

Bisphenol-A polysulfone (PSF) is used commercially as a gas-separation membrane material, and it has a stable aromatic backbone that is amenable to structural modification. The gas pair chosen for this study is the CO₂/CH₄ system. The separation of these gases is of interest in oil recovery, the treatment of landfill gases, sweetening of natural gases, and the greenhouse effect.^{14–16} The permeation properties for a mixture of CO₂ and CH₄ are also measured, and these results are compared with those for pure gases.

This present work is a part of a study of chemical modifications of polysulfone. It is the purpose of this study to investigate the effect of bromo and trimethylsilyl substitutions on the gas-transport properties.

EXPERIMENTAL

Materials and Membrane Preparation

The materials synthesized in this study included bromobisphenol-A polysulfone (BPSF) and BTMSPSF. PSF (Udel® P-3500) was obtained from Amoco Chemical Co. Reagent-grade tetrahydrofuran (THF) was freshly distilled for each reaction.

All other reagents were purchased commercially (Duksan Chemical Co., Korea) and used as received without further purification. The procedure described by Guiver et al.^{17,18} was used for the syntheses of BPSF and BTMSPSF. PSF (0.075 mol, 33.15 g) was dissolved in chloroform (180 mL), and bromine (12 mL) was added to a stirred solution at room temperature. White clouds of HBr soon evolved. The mixture was stirred at room temperature for 24 h and then precipitated into methanol. The recovered brominated polysulfone was reprecipitated several times using THF and methanol to leach out residual-free bromine and then filter-dried in a vacuum oven. Bisphenol-A trimethylsilylated polysulfone (TMSPSF) was synthesized by lithiation and trimethylsilylation (the procedure was discussed in detail¹² in a previous paper). BTMSPSF was synthesized by adding bromine (0.062 mol, 5 g) to a stirred solution of TMSPSF, 0.029 mol, 15 g) in chloroform (60 mL) at room temperature. The resulting solution was stirred for 24 h and then precipitated into methanol, washed, and finally dried to yield BTMSPSF. The recovered polymer was left standing in fresh methanol, then filtered, and dried in a vacuum oven. The chemical structures of modified polysulfones were characterized by ¹H-NMR and ¹³C-NMR and are shown in Figure 1.

The membranes were cast from 10 wt % solution in chloroform on the clean glass plate at room temperature. The membranes were dried under atmosphere for 24 h, controlling the rate of solvent removal. After drying, the membranes were lifted from the glass plate and completely dried in a vacuum oven at 150°C for several days.

Characterization

¹H-NMR and ¹³C-NMR spectra were recorded on a Bruker DRX-500 spectrophotometer. The glass transition temperature (T_g) for each material was measured using a Perkin–Elmer DSC-7 differential scanning calorimeter at a heating rate of 20°C/min. Polymer density was measured using a density gradient column filled with aqueous solutions of calcium nitrate at 23°C. Fractional free volume (FFV) of the polymers was calculated by the group contribution method proposed by Bondi.¹⁹ The wide-angle X-ray diffraction (WAXD) measurements were carried out using Rigaku WAXD-D/MAX III X-ray diffractometer with Cu K α radiation with a wavelength of 1.54 Å. The average intersegmental distances or d spacings

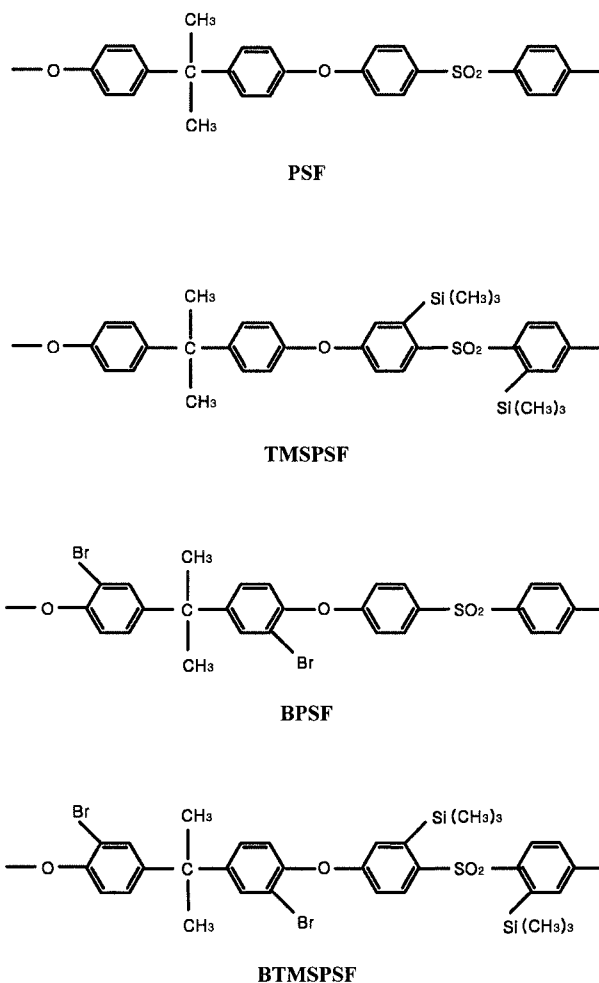


Figure 1 Chemical structures of modified polysulfones.

were calculated from the Bragg equation,²⁰ $n\lambda = 2d \sin \theta$, at the angle of maximum peak of scan. Cohesive energy density (CED) was estimated by the group contributions published by Fedors.¹⁹

Gas Sorption and Permeation

Pure gas-sorption measurements were made for CO₂ and CH₄ up to 25 atm and at 30°C. Equilibrium sorption was measured by the pressure-decay method. The sorption cell is similar to one designed by Koros and Paul,²¹ and described in an earlier paper.²²

Permeability measurements were also made for pure CO₂ and CH₄ and their binary mixture using the apparatus employed in our laboratory.²³ Pure to permeated gas was fed into the upstream side, while the downstream side was filled with the same gas at 1 atm. The volumetric

flow rate through the membrane to the downstream side was determined by observing the displacement of isopropanol in the capillary tube connected to the downstream side. The permeability coefficients were calculated by eq. (1) and (2). Permeation runs were carried out at 30°C and pressures up to 25 atm:

$$P = D \times S = \frac{J_s L}{p_1 - p_2} \quad (1)$$

$$J_s = \frac{\pi d^2}{4A} \frac{273.15 p_b}{76T} \frac{dh}{dt} \quad (2)$$

where P [Barrer, cm³(STP)/cm/cm² s cmHg] is the mean permeability coefficient, D [cm²/s] is the apparent diffusion coefficient, and S [cm³(STP)/cm³ cmHg] is the apparent solubility coefficient. J_s [cm³(STP)/cm² s] is the steady-state rate of gas permeation through unit area when the constant gas pressure p_1 and p_2 are maintained at the membrane interface, and L [cm] is the effective membrane thickness. d [cm] is the diameter of capillary, A [cm²] is the membrane permeation area, p_b [cmHg] is the barometric pressure, T [K] is the experimental temperature, and dh/dt is the displacement rate of propanol in the capillary. The permeation rates for the components of binary gas mixture of CO₂ and CH₄ (CO₂/CH₄ = 57.5/42.5 vol %) were determined by the volumetric flow rate of gas mixture and the concentration of each component on the upstream and downstream side. The concentrations of the components were determined by gas chromatograph (Shimadzu 8A) with a column packed with Porapak Q.

RESULTS AND DISCUSSION

Pure Gas Sorption and Permeation—Dual-Mode Model

Sorption isotherms for CO₂ and CH₄ in BPSF and BTMSPSF are shown in Figures 2 and 3. For each polymer, the pure gas sorption isotherms are concave to the pressure axis and can be described by dual sorption model.²⁴ According to the dual sorption model, the equilibrium concentration of sorbed gas in glassy polymers can be described as a function of pressure:

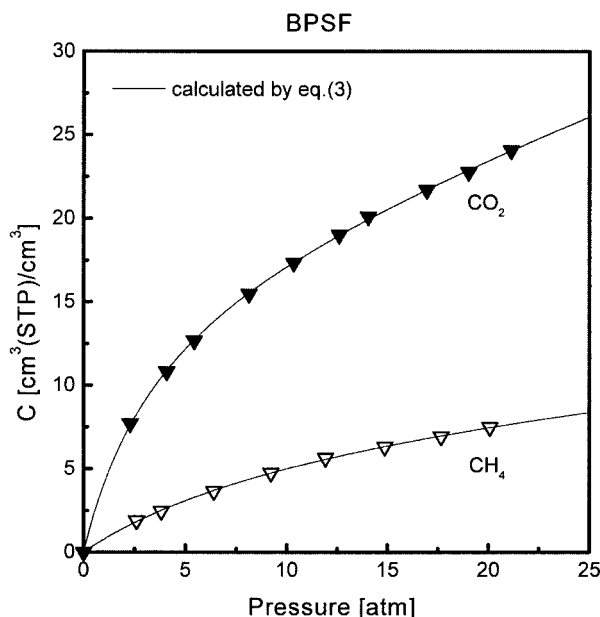


Figure 2 Sorption isotherms for CO₂ and CH₄ in BPSF at 30°C.

$$C = C_D + C_H$$

$$C = k_D p + \frac{C'_H b p}{1 + b p} \quad (3)$$

where C [cm³(STP)/cm³] is the equilibrium concentration of the sorbed gas, and C_D and C_H represent Henry's law-mode sorption and Langmuir-mode sorption, respectively. The parameter k_D [cm³(STP)/cm³ atm] is the Henry's law solubility constant, C'_H [cm³(STP)/cm³] is the Langmuir sorption capacity, and b [atm⁻¹] is the Langmuir affinity constant. These sorption parameters can be obtained by nonlinear least-squares regression and are listed Table I. The solid curves in Figures 2 and 3 represent the dual-mode fits of the actual data, substituting the values of sorption parameters given in Table I. It is shown that the sorption of pure CO₂ and CH₄ are well fitted by the dual sorption model.

The permeability coefficients of pure gases for BPSF and BTMSPSF are shown as a function of upstream pressure in Figures 4 and 5. The permeability coefficients of CO₂ and CH₄ decrease with increasing upstream pressure, as is often the case with other glassy polymers.^{24,25} This pressure-dependency of permeability coefficients were generally described as dual mobility model (or partial immobilization model) proposed by Paul and Koros.^{24,25} According to the dual mobility

model, the populations in each of the sorptions can be assigned separate diffusion coefficients D_D and D_H ; the permeability coefficient of pure gas can be written as:

$$P = k_D D_D \left[1 + \frac{FK}{(1 + b p_1)(1 + b p_2)} \right] \quad (4)$$

where $K = C'_H b / k_D$ and $F = D_H / D_D$. The diffusion coefficients, D_D and D_H , are calculated from the slope and intercept of the plot of experimental permeability coefficient versus $1/(1 + b p_1)(1 + b p_2)$. The diffusion coefficients obtained by this analysis are also listed in Table I. The solid curves in Figures 4 and 5 are calculated by eq. (4) using parameters given in Table I and show that the permeability coefficient is well fitted to dual-mobility model at the entire pressure range.

The Effect of Substituents on Permeation Properties

The comparison of the permeability coefficients of CO₂ and ideal separation factors for modified polysulfones at 10 atm are shown in Table II. The ideal separation factor was calculated from the ratio of the pure component permeability coefficients. The ideal separation factor is the product of diffusivity selectivity (D_{CO_2/CH_4}) and solubility selectivity (S_{CO_2/CH_4}), and the high diffusivity se-

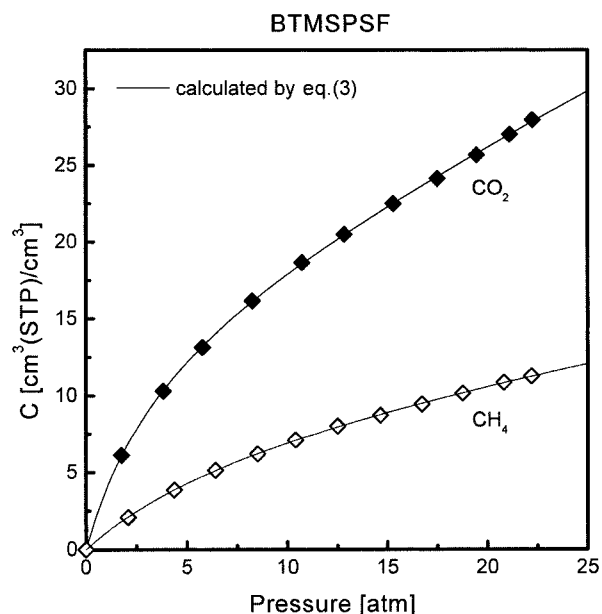


Figure 3 Sorption isotherms for CO₂ and CH₄ in BTMSPSF at 30°C.

Table I Dual Mode Parameters^a for BPSF and BTMSPSF at 30°C

Polymer	Gas	k_D	C'_H	b	D_D	D_H
BPSF	CO ₂	0.429	17.70	0.261	4.718	0.674
	CH ₄	0.096	8.81	0.084	0.652	0.082
BTMSPSF	CO ₂	0.643	15.906	0.257	8.502	0.327
	CH ₄	0.211	9.375	0.105	1.398	0.087

^a Units: k_D [cm³(STP)/cm³ atm]; C'_H [cm³(STP)/cm³]; b (atm⁻¹); $D_D \times 10$ (cm²/s); $D_H \times 10$ (cm²/s).

lectivity in this study results in high ideal separation factor as listed in Table II. In Table II, the data for PSF and TMSPSF¹² in our laboratory are also included to compare with the polymers synthesized in this study. The permeability coefficients of four polysulfones rank in the following order, TMSPSF > BTMSPSF > PSF > BPSF, and ideal separation factors are in the opposite order. The ideal separation factor for BTMSPSF is reduced by about 10% than that for PSF, but BTMSPSF is about two times more permeable than PSF. For BPSF, the ideal separation factor is increased by >20% than that for PSF and is higher than other polysulfones having similar permeability coefficients of CO₂ with BPSF. Figure 6 describes the correlation of ideal separation factors with permeability coefficients of CO₂. Open symbols in Figure 6 represent the results of

polysulfones substituted with other functional groups.^{5,22,26}

In general, the permeation properties depend on intermolecular packing distance, chain stiffness, polymer–polymer interaction, and polymer–penetrant interaction. The physical properties related to permeation properties are listed in Table III. FFV and d spacing have been representative of average intermolecular packing distance or free spaces. FFV, given in Table III, is calculated in eq. (5). The group contribution method of Bondi¹⁹ is used to calculate V_0 , the hypothetical specific volume of the polymer at 0 K; and V , the specific volume of the polymer at T , is determined from the polymer density:

$$\text{FFV} = \frac{V - V_0}{V} \quad (5)$$

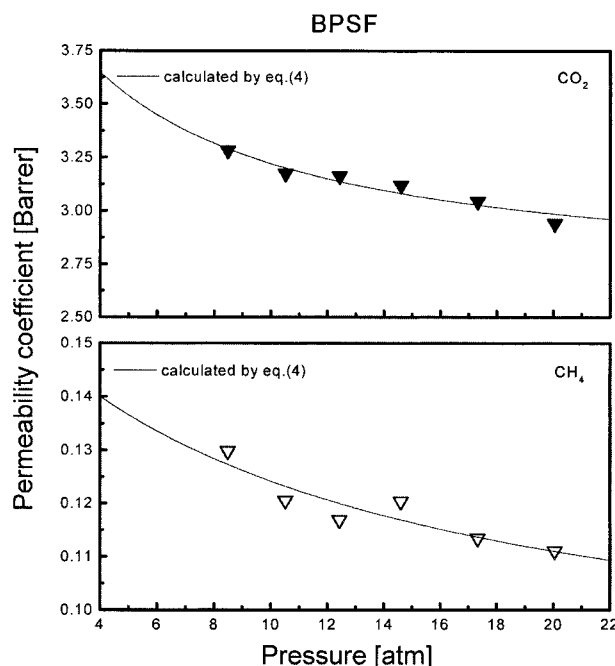


Figure 4 Pressure dependency of permeability coefficients of CO₂ and CH₄ for BPSF at 30°C.

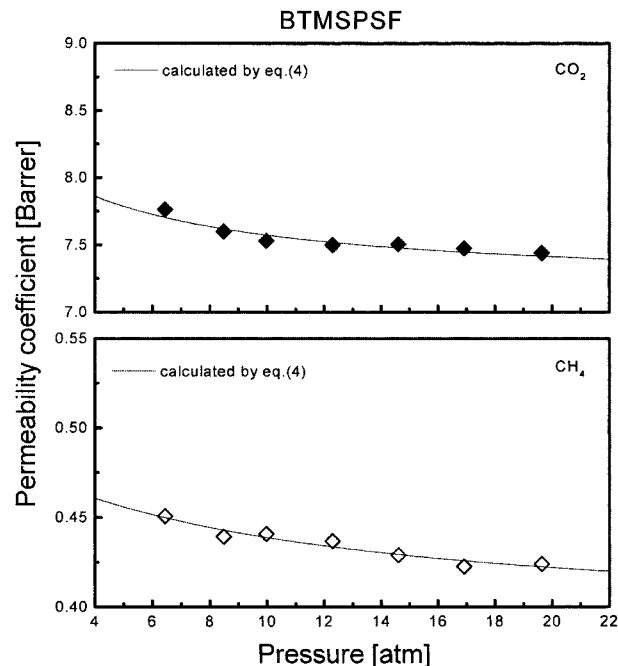


Figure 5 Pressure dependency of permeability coefficients of CO₂ and CH₄ for BTMSPSF at 30°C.

Table II Transport Properties^a of CO₂ and CH₄ for Modified Polysulfones at 30°C and 10 atm

Polymer	P_{CO_2}	$\alpha_{\text{CO}_2/\text{CH}_4}$	S_{CO_2}	$S_{\text{CO}_2/\text{CH}_4}$	D_{CO_2}	$D_{\text{CO}_2/\text{CH}_4}$
PSF ^b	4.6	22	2.4	2.8	1.9	7.8
TMSPSF ^b	15.1	16	2.1	2.7	7.2	5.5
BPSF	3.2	27	1.7	3.4	1.9	7.9
BTMSPSF	8.0	19	2.4	2.8	3.2	6.5

^a Units: $P \times 10^{10}$ [cm³(STP)cm/s cm² cmHg]; $D \times 10^8$ (cm²/s); $S \times 10^2$ [cm³(STP)/cm³ cmHg].

^b Data from ref. 12.

As shown in Tables II and III, the substitutions of bulky trimethylsilyl groups are responsible for the higher FFV of TMSPSF and BTMSPSF. However, BPSF shows the lower value of both permeability coefficient and FFV than PSF. It can be explained that the interchain interaction increased by induced dipole, so the interchain distance is decreased. The higher ideal separation factor BTMSPSF than TMSPSF may be due to the above reason. The addition of bromo substituents to TMSPSF is also found to decrease the permeability coefficients for BTMSPSF, suggesting that the potential increase in FFV due to chain packing—disrupting bulky trimethylsilyl groups is overridden by the increase in interchain interaction. The strong polarity of bromine may act to reduce the chain packing—inhibiting ability.

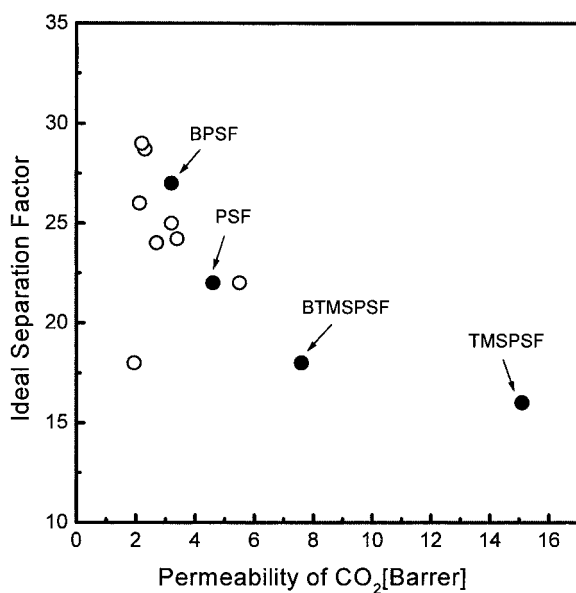


Figure 6 Correlation of ideal separation factor with permeability coefficient for CO₂ at 10 atm and 30°C. Open symbols represent the results of polysulfones substituted with other functional groups.^{5,22,26}

Figure 7 represents the correlation of permeability coefficients with 1/FFV for CO₂ and CH₄. In Figure 7, MSPF (bisphenol-A methylated polysulfone) is the polymer in which ortho sites of sulfone unit in PSF were replaced with methyl groups.²² The correlation between permeability coefficients and 1/FFV is not so clear. For BPSF and BTMSPSF, the deviation may be due to the errors in the estimation of Van der Waals volume, V_W . According to Bondi,²⁷ Van der Waals volumes of the structural elements are estimated with some errors in a situation where bonds may be distorted by dipoles or H bonding. Other workers reported that small errors in the estimation of V_W were found to lead to large differences in calculated FFV.⁷ In addition, McHattie et al.²⁸ and Puleo et al.²⁹ suggested that the increase in intermolecular forces caused by the presence of the polar groups such as halogen results in a lower permeability than would be predicted by estimated FFV. In some polymers, the gas-permeability coefficient was correlated with d spacing.^{30–32} The variation of d spacing in this work is reasonably consistent with the permeability coefficient. For example, TMSPSF has the highest d spacing and permeability coefficient, and BPSF the lowest values. BPSF and BTMSPSF have additional peaks corresponding to 9.5 and 10.4 Å, respectively, as shown in Table II. Aguilar-Vega and Paul³³ and Jacobson³⁴ reported that the appearance of the second peak might stem from the intrachain interaction. A more careful study of this result is needed to elucidate the intrachain interaction corresponding to the second peak.

It is generally known that the T_g is a pragmatic measure of the chain stiffness of polymer backbone, and chain stiffening leads to high permselectivity.^{35,36} In our study, the values of T_g of silylated polysulfones are more than 20°C lower than that of PSF. This result may be due to the flexible C—Si bond and increase of free vol-

Table III Physical Properties for Modified Polysulfones

Polymer	T_g (°C)	ρ (g/cm ³)	d Spacing (Å)	δ (cal/cm ³) ^{1/2}	FFV
PSF ^a	190.3	1.243	5.2	12.4	0.158
TMSPSF ^a	164.0	1.126	5.6	11.0	0.167
BPSF	190.9	1.514	4.7 (9.5)	12.9	0.156
BTMSPSF	169.5	1.244	5.3 (10.4)	11.5	0.168

^a Data from ref. 12.

ume. The lower ideal separation factors of these polysulfones may be attributed, at least in part, to the lower T_g of these polymers.

CED is also an important factor for prediction of structure-selectivity relationships. The higher the CED, the higher the attractive forces between polymer chains. This means that the permselectivity will tend to be higher for polar polymers than nonpolar polymers. CED is usually expressed in terms of solubility parameter δ [(cal/cm³)^{1/2}], where $\delta = (\text{CED})^{1/2}$, and the values of the solubility parameter are listed in Table III. Figure 8 represents the correlation of ideal separation factors at 10 atm with solubility parameters of polysulfones in this study. The polysulfone with higher δ has the higher ideal separation factor. The higher ideal separation factors of BPSF and BTMSPSF in comparison with PSF and TMSPSF,

respectively, are due to the polarity of bromine as discussed above.

Mixed Gas Permeation

The gas permeation and separation property studies were especially focused on glassy polymers because of their superior gas selectivities in comparison to rubbery polymers. The presence of unrelaxed volume in a glassy polymer plays an important role in controlling the gas permeation rate and, thereby, the separation of two or more components. However, the use of single gas-permeation data to estimate the separation properties of such a membrane can lead to erroneous results.^{37,38} In this study, the permeation properties for a mixture of CO₂ and CH₄ were measured, and these results were compared with those ob-

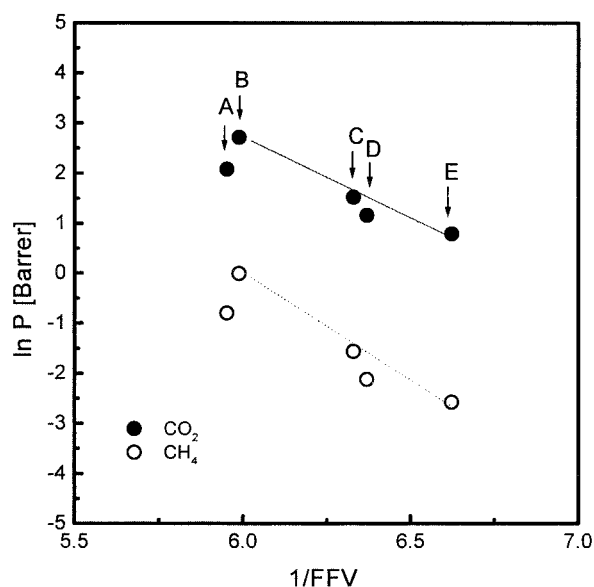


Figure 7 Correlation of permeability coefficients at 10 atm and 30°C with inverse fractional free volume of modified polysulfones; A = BTMSPSF, B = TMSPSF, C = PSF, D = BPSF, and E = MPSF.

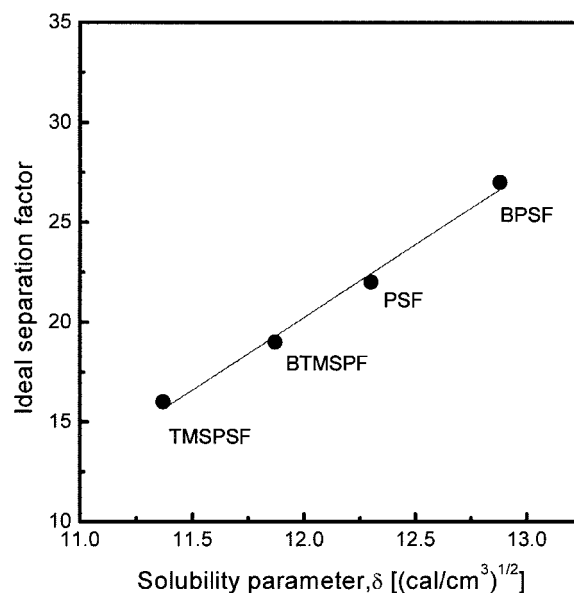


Figure 8 Correlation of ideal separation factors at 10 atm and 30°C with solubility parameters of modified polysulfones.

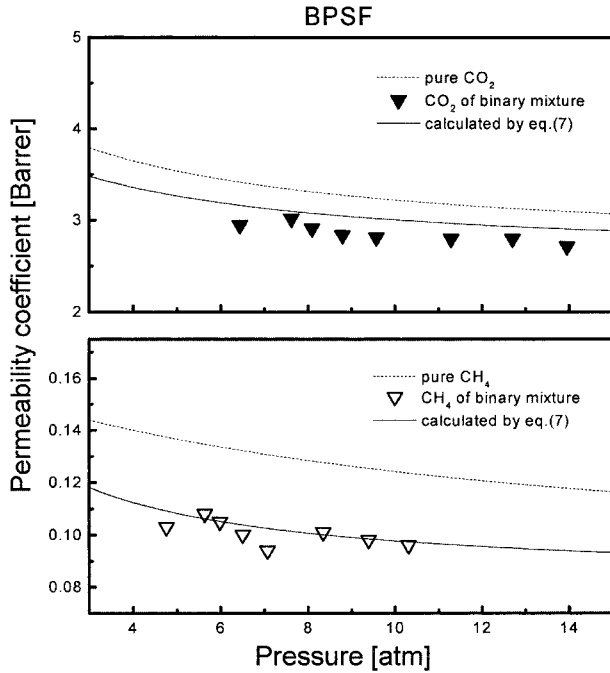


Figure 9 Permeability coefficients for CO₂ and CH₄ in a binary mixture for BPSF at 30°C.

tained from the experiments of pure gases. The permeability coefficients of CO₂ and CH₄ in a binary mixture (CO₂/CH₄ = 57.5/42.5 vol %) for BPSF and BTMSPSF are illustrated in Figures 9 and 10. The dashed curves in Figures 9 and 10 represent the values calculated from pure gas data by eq. (4) based on the respective partial pressures, and which is to compare mixed gas permeabilities with the values of pure gases at the same partial pressure. For each polymer, mixed gas-permeability coefficients are lower than the respective pure component values. Such a reduction in permeability coefficient in binary mixture is commonly observed in other polymers.^{5,38} On the basis of the dual-mode model for pure gas, Koros³⁹ extended the model to the case of gas mixtures in glassy polymers. For cases involving only weak penetrant–penetrant and penetrant–polymer interactions, Koros³⁹ assumed that the primary effect of a mixture is competition by the various penetrants for the fixed unrelaxed volume in the polymer, and that diffusivity of a penetrant in the polymer is not changed much by introducing a second component. For component A in the binary mixture, the concentration of sorbed gas and permeability coefficient can be written as:

$$C_A = k_{DA}p_A + \frac{C'_{HA}b_{AP_A}}{1 + b_{AP_A} + b_{BP_B}} \quad (6)$$

$$P_A = k_{DA}D_{DA} \left[1 + F_A K_A \frac{(b_{BP_{A1}}p_{B2} - b_{BP_{A2}}p_{B1})}{p_{A1} - p_{A2}} \right] \times \frac{1}{(1 + b_{AP_{A1}} + b_{BP_{B1}})(1 + b_{AP_{A2}} + b_{BP_{B2}})} \quad (7)$$

where subscripts A and B represent components A and B, and all the parameters are obtained by pure gas experiment. The solid curves in Figures 9 and 10 represent the values calculated from pure gas data by eq. (7) and show that the permeability coefficient in a binary mixture is reasonably well fitted to the dual-mobility model for a binary gas mixture. As the above assumption suggested by Koros, the permeability depression in Figures 9 and 10 is due to the solubility effect and the result from the competition between CO₂ and CH₄ for the Langmuir sites in glassy polymers.

The separation factor, α , is defined as

$$\alpha_{(A/B)} \equiv \frac{y_A/y_B}{x_A/x_B} \quad (8)$$

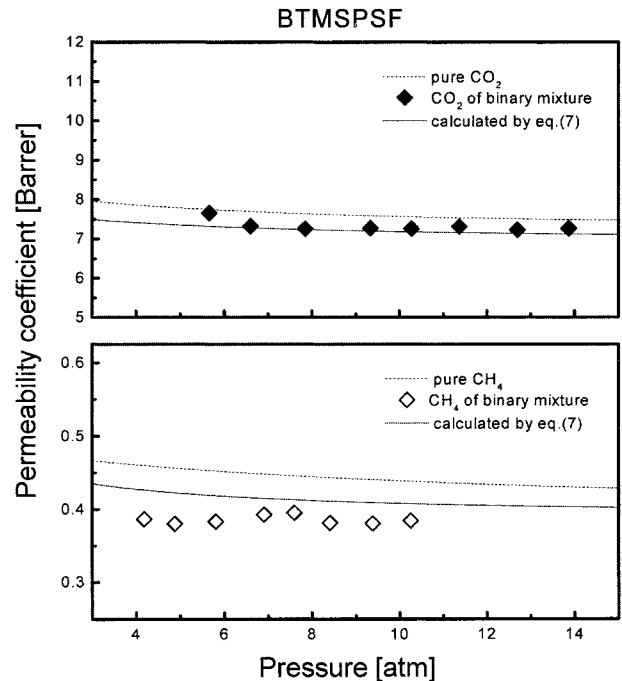


Figure 10 Permeability coefficients for CO₂ and CH₄ in a binary mixture for BTMSPSF at 30°C.

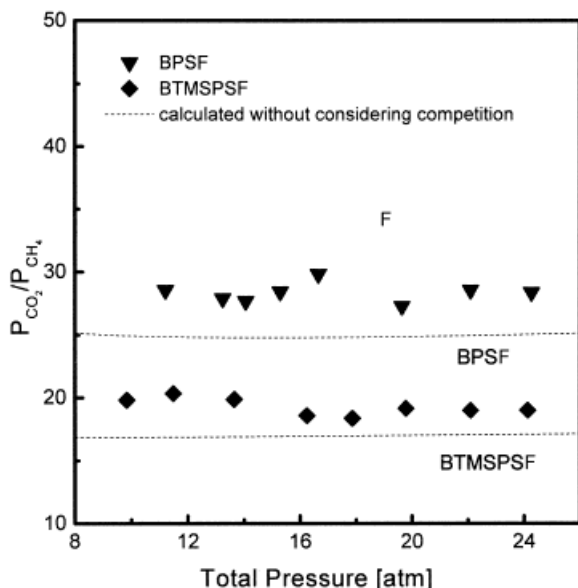


Figure 11 Separation factors of CO₂ and CH₄ in a binary mixture for BPSF and BTMSPSF at 30°C. Dashed lines represent calculated values without considering competition effect.

where y_i 's and x_i 's are the mole fractions of the components in the downstream and upstream, respectively. When the pressure of the downstream is very small compared with the upstream pressure, the separation factor will be approximately equal to the ratio of permeabilities in a binary mixture. Figure 11 represents the separation factors obtained by the ratio of mixed gas permeabilities. The dashed curves in Figure 11 correspond to calculated values by eq. (4), without considering the competition effect. The mixed gas permselectivity is higher than the pure gas value, which also shows the competition effect between each component. For each polymer, the value of Langmuir affinity constant, b , for CO₂ is higher than for CH₄, so the depression of the permeability coefficient of CH₄ in a binary gas mixture is higher than that of CO₂, as explained by eqs. (6) and (7). Therefore, the separation factor of a mixed gas is higher than the value without considering competition effect.

CONCLUSIONS

The effects of molecular structure of polysulfones on transport properties are studied using chemically modified polysulfones, including TMSPSF, BPSF, and BTMSPSF. The substitution of very bulky trimethylsilyl groups shows the strong ef-

fect on chain packing and stiffness. The replacement of phenylene hydrogens of PSF with trimethylsilyl groups results in increases in interchain distance and decreases in chain stiffness. Silylated polysulfones are several times more permeable than PSF. The higher values of permeability coefficient for TMSPSF and BTMSPSF are due to higher chain packing distance by the addition of bulky substituents. The substitution of bromines results in higher chain interactions, judged by the value of cohesive energy density, and lower interchain distance. The strong polarity of bromine reduces the chain packing-inhibiting ability. BPSF is less permeable than PSF, but is more permselective. Substitution of bromines to TMSPSF is also found to decrease the permeability coefficients for BTMSPSF, suggesting that the potential increase in FFV and d spacing due to bulky trimethylsilyl groups is overridden by the increase in interchain interaction. The permeability coefficients for each gas of a binary mixture are lower than the respective values of pure gases, which represents the competition effect for permeation of mixed gas. The extent of such a depression is larger for CH₄, having a lower value of the Langmuir affinity constant.

NOMENCLATURE

A	permeation area [cm ²]
b	Langmuir affinity constant [atm ⁻¹]
C	concentration of sorbed gas [cm ³ (STP)/cm ³]
C'_H	Langmuir sorption constant [cm ³ (STP)/cm ³]
D	diffusion coefficient [cm ² /s]
d	capillary diameter [cm]
h	height [cm]
J_S	steady-state diffusion flux [cm ³ (STP)/cm ² s]
k_D	Henry's law solubility constant [cm ³ (STP)/cm ³ atm]
L	membrane thickness [cm]
P	permeability coefficient [cm ³ (STP)cm/cm ² s cmHg]
p	pressure [atm]
p_b	barometric pressure [atm]
S	solubility coefficient [cm ³ (STP)/cm ³ atm]
T	temperature [K]
t	time [s]
V	specific volume [cm ³]
x	mole fraction of upstream
y	mole fraction of downstream

Greek Symbols

- α separation factor
 δ solubility parameter $[(\text{cal}/\text{cm}^3)^{1/2}]$

Subscripts

- A* component *A*
B component *B*
D Henry's law mode
H Langmuir mode
 1 upstream face of the membrane
 2 downstream face of the membrane

REFERENCES

- Stern, S. A. *J Membr Sci* 1994, 94, 1.
- Koros, W. J.; Fleming, G. K. *J Membr Sci* 1993, 83, 1.
- McHattie, J. S.; Koros, W. J.; Paul, D. R. *Polymer* 1991, 32, 840.
- Houde, A. Y.; Kulkarni, S. S.; Kharul, U. K.; Charati, S. G.; Kulkarni, M. G. *J Membr Sci* 1995, 103, 167.
- Ghosal, K.; Chern, R. T.; Freeman, B. D.; Daly, W. H.; Negulescu, I. I. *Macromolecules* 1996, 29, 4360.
- Pixton, M. R.; Paul, D. R. *Polymer* 1995, 36, 3165.
- Ghosal, K.; Freeman, B. D.; Chern, R. T.; Alvarez, J. C.; de la Campa, J. G.; Lozano, A. E.; de Abajo, J. *Polymer* 1995, 36, 793.
- Kim, T. H.; Koros, W. J.; Husk, G. R.; O'Brien, K. C. *J Membr Sci* 1988, 37, 45.
- Aitken, C. L.; Koros, W. J.; Paul, D. R. *Macromolecules* 1992, 25, 3424.
- Mulder, M. in *Basic Principles of Membrane Technology*; Kluwer Academic: Dordrecht, The Netherlands, 1991, pp 17–53.
- Ichiraku, Y.; Stern, S. A.; Nakagawa, T. *J Membr Sci* 1987, 34, 5.
- Kim, H. J.; Hong, S. I. *Korean J Chem Eng* 1997, 14, 382.
- Muruganandam, N.; Koros, W. J.; Paul, D. R. *J Polym Sci, Part B: Polym Phys* 1987, 25, 1999.
- Bhide, B. D.; Stern, S. A. *J Membr Sci* 1993, 81, 209.
- Bollinger, W. A.; MacLean, D. L.; Narayan, R. S. *Chem Eng Prog* 1982, Oct, 27.
- Rautenbach, R.; Welsch, K. *J Membr Sci* 1994, 87, 107.
- Guiver, M. D.; Kutow, O.; ApSimon, J. W. *Polymer* 1989, 30, 1137.
- Guiver, M. D.; ApSimon, J. W.; Kutow, O. U.S. Pat. 4,797,457, 1989.
- Van Krevelen, D. W. in *Properties of Polymers*; Elsevier: Amsterdam, The Netherlands, 1990; pp 71–107.
- Balta-Calleja, F. J.; Vonk, C. G. in *X-ray Scattering of Synthetic Polymers*; Elsevier: Amsterdam, The Netherlands, 1989; pp 1–31.
- Koros, W. J.; Paul, D. R. *J Polym Sci, Part B: Polym Phys Ed* 1976, 14, 1903.
- Kim, H. J.; Hong, S. I. *Korean J Chem Eng* 1997, 14, 168.
- Hong, S. I.; Kim, H. J.; Park, H. Y.; Kim, T. J.; Jeong, Y. S. *J Korean Ind Eng Chem* 1996, 7, 877.
- Koros, W. J.; Chern, R. T. in *Handbook of Separation Process*; Rousseau, R. W., Ed.; Wiley-Interscience: New York, 1987; pp 862–953.
- Paul, D. R.; Koros, W. J. *J Polym Sci, Part B: Polym Phys Ed* 1976, 14, 675.
- Ghosal, K.; Chern, R. T. *J Membr Sci* 1992, 72, 91.
- Bondi, A. *J Phys Chem* 1964, 68, 441.
- McHattie, J. S.; Koros, W. J.; Paul, D. R. *J Polym Sci, Part B: Polym Phys Ed* 1991, 29, 731.
- Puleo, A. C.; Muruganadam, N.; Paul, D. R. *J Polym Sci, Part B: Polym Phys Ed* 1989, 27, 2385.
- O'Brien, K. C.; Koros, W. J.; Husk, G. R. *J Membr Sci* 1988, 35, 217.
- Hellums, M. W.; Koros, W. J.; Husk, G. R.; Paul, D. R. *J Membr Sci* 1989, 46, 93.
- Charati, S. G.; Houde, A. Y.; Kulkarni, S. S.; Kulkarni, M. G. *J Polym Sci, Part B: Polym Phys Ed* 1991, 29, 921.
- Aguilar-Vega, M.; Paul, D. R. *J Polym Sci, Part B: Polym Phys Ed* 1993, 31, 1577.
- Jacobson, S. H. *Polym Prepr* 1991, 32, 39.
- McHattie, J. S.; Koros, W. J.; Paul, D. R. *Polymer* 1991, 32, 2618.
- McHattie, J. S.; Koros, W. J.; Paul, D. R. *Polymer* 1992, 33, 1701.
- Dhingra, S. S.; Marand, E. *J Membr Sci* 1998, 141, 45.
- Chern, R. T.; Koros, W. J.; Yuri, B.; Hopenberg, H. B.; Stanett, V. T. *J Polym Sci, Part B: Polym Phys Ed* 1984, 22, 1061.
- Koros, W. J. *J Polym Sci, Part B: Polym Phys Ed* 1980, 18, 981.